Charm Physics at BESIII *

Hailong Ma (For BESIII Collaboration)

Institute of High Energy Physics, Chinese Academy of Sciences, Beijing, 100049, China

Abstract: Based on 2.93 and 0.567 fb^{-1} data taken at the center-of-mass energies $\sqrt{s}$ = 3.773 and 4.599 GeV with the BESIII detector, we report the precise measurements of the decay constant f_{D^+}, the form factors of D semileptonic decays, the Dalitz plot analysis of $D^+ \to K^0_S\pi^+\pi^0$, the strong phase differences in $D \to K^0_{S/L}\pi^+\pi^-$ and $K^-\pi^+$, the $D^0\bar{D}^0$ mixing parameter $y_{\rm CP}$, the searches for 2-body hadronic decays $D^{0(+)} \to \omega\pi^{0(+)}$, rare decays of $D^0 \to \gamma\gamma$ and $D^+ \to K(\pi)^\pm e^\mp e^+$ as well as the significant improved measurements of the absolute branching fractions for $\Lambda_c^+ \to \Lambda e^+\nu_e$ and 12 hadronic final states.

Key words: charmed meson and baryon, leptonic and semileptonic decays, hadronic decay, decay constant, form factor, strong phase, quark mixing matrix element

PACS: 12.20.Fc, 12.15.Hh, 14.40.Lb, 14.20.Lq

BESIII粲物理
马海龙

中国科学院高能物理研究所，100049，中国北京

Abstract: 分析BESIII探测器在质心系能量3.773和4.599 GeV采集的2.93和0.567 fb^{-1}数据，我们报道了衰变常数f_{D^+}和D介子半轻子衰变的形状因子，$D^+ \to K^0_S\pi^+\pi^0$的Dalitz图分析，$D \to K^0_{S/L}\pi^+\pi^-$和$K^-\pi^+$强相差，$D^0\bar{D}^0$混合参数$y_{\rm CP}$的测量；2体强子衰变$D^{0(+)} \to \omega\pi^{0(+)}$，稀有衰变$D^0 \to \gamma\gamma$和$D^+ \to K(\pi)^\pm e^\mp e^+$的寻找；以及$\Lambda_c^+ \to \Lambda e^+\nu_e$和12个强子衰变绝对分支比的测量。

Key words: 粲介(重)子，纯轻和半轻子衰变，强子衰变，稀有衰变，衰变常数，形状因子，强相角，夸克混合矩阵

1 Introduction

Precision measurements of charm decays provide rich information to better understand strong and weak effects. Firstly, the (deferential) decay rates of the D leptonic and semileptonic decays can be simply functioned as decay constant f_{D^+} or form factors and CKM matrix element $|V_{cs(d)}|$. From analysis of the D leptonic and semileptonic decays, we can determine these elementary constants, thus calibrating the LQCD calculation on f_{D^+} and the form factors and testing the CKM matrix unitarity.

Secondly, studies of D hadronic decays are important due to several aspects. At $\psi(3770)$, the quantum correction property of D^0 meson production provides an access to CP asymmetry in $D^0\bar{D}^0$ mixing and strong phase parameters which can be used to constrain γ/ϕ_3 and to further test the CKM matrix unitarity. Improved knowledge of 2-body decays is helpful for understanding of U-spin and $SU(3)$ flavor symmetry breaking effects. Datlitz plot analysis of 3-body decays can provide rich information about the parameters of sub-resonances and strong phases.

Thirdly, in the Standard Model (SM), the Flavor Changed Neutral Current (FCNC) process and the Leptonic Number Violation (LNV) process are highly suppressed. However, some new dynamics beyond the SM may enhance these kinds of processes to observable level at BESIII. So, search for these rare decays can be used to probe for new physics beyond the SM. Any evidence of rare decay and CP violation in charm decays or significant deviation of CKM unitarity may indicate new physics beyond the SM.

Finally, compared to charmed meson decays, the knowledge of charmed baryon Λ_c^+ decays is still very poor. It is desired to improve the measurements of the known decays and search for new decay modes. Significantly improved knowledge of the decay rates or dynmics of charm decays can also provide better inputs for beauty physics.

Received November 30, 2015

∗ I would like to thank for the support of the National Natural Science Foundation of China (NSFC) under Contracts No. 10935007 and No. 11305180, and the Ministry of Science and Technology of China (973 by MOST) under Contracts No. 2009CB825200 and No. 2015CB856700.

Herein, we report recent results on the studies of the leptonic, semleptonic and hadronic decays of D^0, D^+ and Λ_c^+. These are based on 2.93 [2] and 0.567 [3] fb^{-1} data at $\sqrt{s}$ = 3.773 and 4.599 GeV, where $D^0\bar{D}^0$, D^+D^- and $\Lambda_c^+\bar{\Lambda}_c^-$ are produced in pairs, taken with the BESIII detector [1]. Throughout the proceeding, charge conjugate is implied.

2 D leptonic and semileptonic decay

In the Standard Model, the D^+ mesons decay into $\ell\nu_\ell$ via a virtual W^+ boson. The decay rate of the leptonic decays $D^+ \to \ell^+\nu_\ell$ can be parameterized by the D^+ decay constant f_{D^+} via

$$\Gamma(D^+ \to \ell^+\nu_\ell) = \frac{G_F^2}{8\pi}|V_{cd}|^2 f_{D^+}^2 m_\ell^2 m_{D^+}(1-\frac{m_\ell^2}{m_{D^+}^2}), \quad (1)$$

where G_F is the Fermi coupling constant, $|V_{cd}|$ is the quark mixing matrix element, m_ℓ and m_{D^+} are the lepton and D^+ masses. To investigate the leptonic decay $D^+ \to \mu^+\nu_\mu$ [4], the singly tagged D^- mesons are reconstructed using 9 hadronic decays $K^+\pi^-\pi^-$, $K_S^0\pi^-$, $K_S^0K^-$, $K^+K^-\pi^-$, $K^+\pi^-\pi^-\pi^0$, $\pi^+\pi^-\pi^-$, $K_S^0\pi^-\pi^0$, $K^+\pi^+\pi^-\pi^-\pi^-$ and $K_S^0\pi^+\pi^-\pi^-$. From these, we accumulate (170.31±0.34)×10^4 singly tagged D^- mesons. Fig. 1 (Left) shows the $M^2_{\rm miss}$ distribution of the $D^+ \to \mu^+\nu_\mu$ candidates, which are selected in the systems against the singly tagged D^- mesons. We obtain 409±21 $D^+ \to \mu^+\nu_\mu$ signals after background subtraction, which leads to the branching fraction $\mathcal{B}(D^+ \to \mu^+\nu_\mu) = (3.71 \pm 0.19_{\rm stat.} \pm 0.06_{\rm sys.}) \times 10^{-4}$. Using the measured $\mathcal{B}(D^+ \to \mu^+\nu_\mu)$ and the quark mixing matrix element $|V_{cd}|$ from a global Standard Model fit [5], we determine the D^+ decay constant $f_{D^+} = 203.2 \pm 5.3_{\rm stat.} \pm 1.8_{\rm sys.}$ MeV. Fig. 1 (Right) compares the f_{D^+} measured at BESIII and CLEO [6] as well as those calculated by recent theories. The $\mathcal{B}(D^+ \to \mu^+\nu_\mu)$ and f_{D^+} measured at BESIII are consistent within errors with previous measurements, but with the best precision. By using the measured $B(D^+ \to \mu^+\nu_\mu)$ and the LQCD calculation on f_{D^+} [7], we determine $|V_{cd}| = 0.2210 \pm 0.058_{\rm stat.} \pm 0.047_{\rm sys.}$, which has the best precision in the world to date.

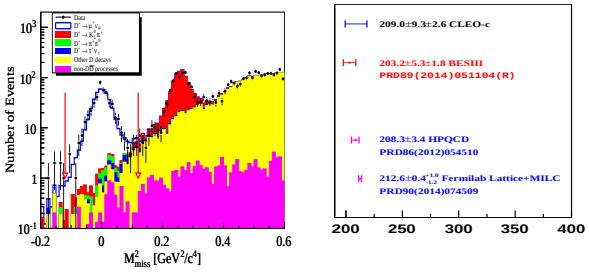

Fig. 1. (Left) $M^2_{\rm miss}$ distribution of the $D^+ \to \mu^+\nu_\mu$ candidates. (Right) Comparison of f_{D^+}.

On the other hand, the D semileptonic decays can be parameterized by the quark mixing matrix element and the form factor of hadronic weak current simply, thus providing an ideal window to probe for the weak and strong effects. For example, the differential decay rates of $D \to K(\pi)e^+\nu_e$ can be simply written as

$$\frac{d\Gamma}{dq^2} = \frac{G_F^2}{24\pi^3}|V_{cs(d)}|^2 p^3_{K(\pi)}|f_+^{K(\pi)}(q^2)|^2, \quad (2)$$

where G_F is the Fermi coupling constant, $|V_{cs(d)}|$ is the quark mixing matrix element, $p_{K(\pi)}$ is the kaon(pion) momentum in the D^0 rest frame, $f_+^{K(\pi)}(q^2)$ is the form factor of hadronic weak current depending on the square of the four momentum transfer $q = p_D - p_{K(\pi)}$. To investigate the semileptonic decays $D^0 \to K(\pi)^-e^+\nu_e$ [8], we reconstruct the singly tagged $\bar{D}^0$ mesons using 5 hadronic decays of $K^+\pi^-$, $K^+\pi^-\pi^0$, $K^+\pi^-\pi^-\pi^+$, $K^+\pi^-\pi^-\pi^+\pi^0$ and $K^+\pi^-\pi^0\pi^0$, which give $(279.33 \pm 0.37) \times 10^4$ singly tagged $\bar{D}^0$ mesons. Base on 70727 ± 278 $D^0 \to K^-e^+\nu_e$ and 6297 ± 87 and $D^0 \to \pi^-e^+\nu_e$ signals, we determine the branching fractions $\mathcal{B}(D^0 \to K^-e^+\nu_e) = (3.505 \pm 0.014_{\rm stat.} \pm 0.033_{\rm sys.})\%$ and $\mathcal{B}(D^0 \to \pi^-e^+\nu_e) = (0.2950 \pm 0.0041_{\rm stat.} \pm 0.0026_{\rm sys.})\%$, respectively. The branching fractions measured at BESIII are consistent within errors with previous measurements, but with the best precision. Fig. 2 shows the fits to the partial widths for $D^0 \to K^-e^+\nu_e$ and $D^0 \to \pi^-e^+\nu_e$ using the Simple Pole model [9], the Modified Pole model [9], the two-parameter series expansion (Series.2.Par.) [10] and the three-parameter series expansion (Series.3.Par.) [10]. From the fits, we obtain the parameters of different models. With the extracted $f_+^{K(\pi)}(0)|V_{cs(d)}|$ based on two-parameter series expansion and the expected $f_+^{K(\pi)}(0)$ by LQCD [11, 12], we determine the quark mixing matrix elements $|V_{cs(d)}|$. Fig. 3 compares the $|V_{cs(d)}|$ extracted at BESIII with the ones from different experiments.

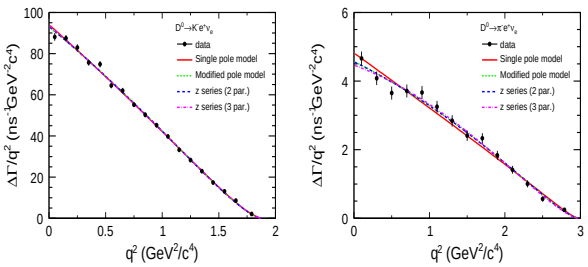

Fig. 2. Fits to the partial widths of (Left) $D^0 \to K^-e^+\nu_e$ and (Right) $D^0 \to \pi^-e^+\nu_e$.

To study the semileptonic decays $D^+ \to K_L^0e^+\nu_e$, $D^+ \to K^-\pi^+e^+\nu_e$ and $D^+ \to \omega(\phi)e^+\nu_e$, we use 6 hadronic decays of $K^+\pi^-\pi^-$, $K^+\pi^-\pi^-\pi^0$, $K_S^0\pi^-$, $K_S^0\pi^-\pi^0$, $K_S^0\pi^+\pi^-\pi^-$ and $K^+K^-\pi^-$. With about 24 thousands of $D^+ \to K_L^0e^+\nu_e$ signals [13], we make first measurement of the branching fraction $\mathcal{B}(D^+ \to$

$K_L^0 e^+\nu_e) = (4.482 \pm 0.027_{\rm stat.} \pm 0.103_{\rm sys.})\%$ and the CP asymmetry $A_{\rm CP}^{D^+\to K_L^0 e^+\nu_e} = (-0.59 \pm 0.60_{\rm stat.} \pm 1.50_{\rm sys.})\%$, supporting that there is no CP asymmetry in this decay. In addition, we perform simultaneous fit to the event density $I(q^2)$ for different tag modes with the two-parameter series expansion and obtain the product of $f_+^K(0)|V_{cs}| = 0.728 \pm 0.006_{\rm stat.} \pm 0.011_{\rm sys.}$.

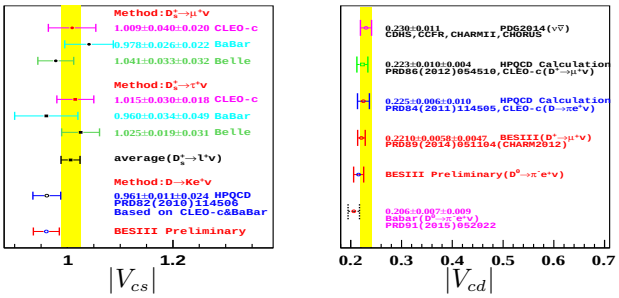

Fig. 3. Comparison of the extracted (Left) $|V_{cs}|$ and (Right) $|V_{cd}|$ based on different experiments.

Using 18262 $D^+ \to K^-\pi^+e^+\nu_e$ candidates [14] which is almost background free, we determine the branching fraction $\mathcal{B}(D^+ \to K^-\pi^+e^+\nu_e) = (3.71 \pm 0.03 \pm 0.08)\%$. A partial wave analysis (PWA) is performed on the selected candidates, with results shown in Fig. 4. The PWA results show that the dominant $\bar{K}^{*0}$ component is accompanied by an S-wave contribution accounting for $(6.05 \pm 0.22 \pm 0.18)\%$ of the total rate, and other components can be negligible. We obtain the mass and width of $\bar{K}^{*0}(892)$ $M_{\bar{K}^{*0}(892)} = (894.60 \pm 0.25 \pm 0.08)$ MeV/c^2 and $\Gamma_{\bar{K}^{*0}(892)} = (46.42 \pm 0.56 \pm 0.15)$ MeV/c^2, the Blatt-Weisskopf parameter $r_{\rm BW} = 3.07 \pm 0.26 \pm 0.11$ (GeV/c)$^{-1}$, as well as the parameters of the hadronic form factors $r_V = \frac{V(0)}{A_1(0)} = 1.411 \pm 0.058 \pm 0.007$, $r_2 = \frac{A_2(0)}{A_1(0)} = 0.788 \pm 0.042 \pm 0.008$, $m_V = (1.81^{+0.25}_{-0.17} \pm 0.02)$ MeV/c^2, $m_A = (2.61^{+0.22}_{-0.17} \pm 0.03)$ MeV/c^2, $A_1(0) = 0.585 \pm 0.011 \pm 0.017$. In the above PWA process, the phase of the non-resonant background $\delta_S(m_{K\pi})$ is factorized by the LASS parameterizations, and the helicity form factors $H_+(q^2, m_{K\pi})$, $H_-(q^2, m_{K\pi})$ and $H_0(q^2, m_{K\pi})$ are parameterized by the spectroscopic pole dominance (SPD) model [15, 16]. We also make model-independent measurements of the $\delta_S(m_{K\pi})$, and the helicity form factors, respectively. The results are consistent with the expectations of the corresponding models and previous measurements.

Based on 491 ± 32 $D^+ \to \omega e^+\nu_e$ signals [17], we determine the branching fraction $\mathcal{B}(D^+ \to \omega e^+\nu_e) = (1.63 \pm 0.11_{\rm stat.} \pm 0.08_{\rm sys.}) \times 10^{-3}$, which is consistent with previous measurements but with better precision. We perform amplitude analysis of $D^+ \to \omega e^+\nu_e$ for the first time, and obtain the ratios of the hadronic form factors to be $r_V = \frac{V(0)}{A_1(0)} = 1.24 \pm 0.09_{\rm stat.} \pm 0.06_{\rm sys.}$ and $r_2 = \frac{A_2(0)}{A_1(0)} = 1.05 \pm 0.15_{\rm stat.} \pm 0.05_{\rm sys.}$. Also, we search for $D^+ \to \phi e^+\nu_e$, but do not find obvious signal. So, we set the upper limit on the branching fraction for $D^+ \to \phi e^+\nu_e$ to be 1.3×10^{-5} at 90% Confidence Level, which is significantly better than previous searches.

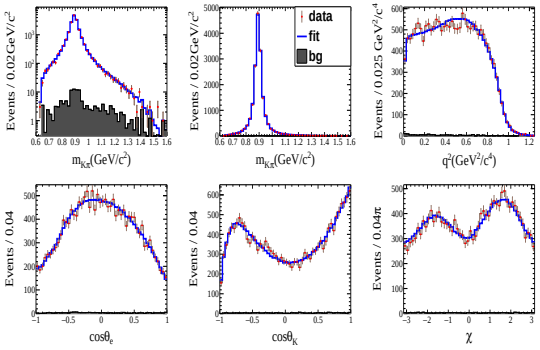

Fig. 4. Projections of the kinematic variables of PWA for $D^+ \to K^-\pi^+e^+\nu_e$, where $m_{K\pi}$ is the $K\pi$ mass, q^2 is the $e\nu_e$ mass square, θ_K is the angle between π and D momenta in the $K\pi$ rest frame, θ_e is the angle between ν_e and D momenta in the $e\nu_e$ rest frame and χ is the angle between the two decay planes. The dots with error bars are data, the blue curves are the weighted signal MC and the hatched histograms are the simulated backgrounds.

3 D hadronic decays

We perform Dalitz plot analysis on the 3-body decay $D^+ \to K_S^0\pi^+\pi^0$ [18]. Based on 166694 candidate events with a background of about 15%, we fit the distribution of data to a coherent sum of six intermediate resonances plus a nonresonant component with a low mass scalar resonance $\bar{\kappa}$ included, with results shown in Fig. 6. From the analysis, we obtain the fitted fraction for each component.

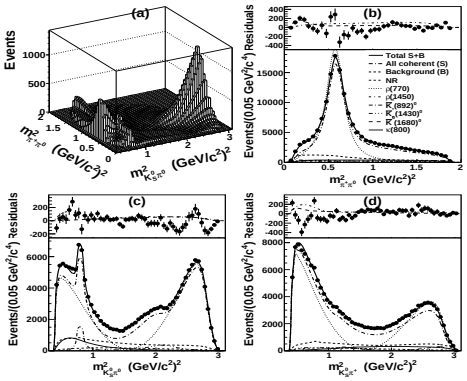

Fig. 5. The results of fitting the $D^+ \to K_S^0\pi^+\pi^0$ data (a) Distribution of fitted p.d.f. and projections on (b) $m^2_{\pi^+\pi^0}$, (c) $m^2_{K_S^0\pi^0}$ and (d) $m^2_{K_S^0\pi^+}$. Residual between the data and total p.d.f are shown by dots with statistical error bars in the top insets with minor contributions from the $\rho(1450)^+$ and the $\bar{K}^*(1680)^0$.

Combing the fitted fractions and the world averaged branching fraction for $D^+ \to K^0_S\pi^+\pi^0$ (6.99±0.27)% [19], we obtain the partial branching fractions as summarized in Tab. 1.

Table 1. Summary of the partial branching fractions, where the uncertainties are statistical, experimental systematic and modeling systematic, respectively.

$D^+ \to$	Partial $\mathcal{B}$ (%)
$K^0_S\pi^+\pi^0$ nonresonance	$0.32\pm0.05\pm0.25^{+0.28}_{-0.25}$
$\rho^+K^0_S, \rho^+ \to \pi^+\pi^0$	$5.83\pm0.16\pm0.30^{+0.45}_{-0.15}$
$\rho(1450)^+K^0_S, \rho(1450)^+ \to \pi^+\pi^0$	$0.15\pm0.02\pm0.09^{+0.07}_{-0.11}$
$\bar{K}^*(892)^0\pi^+, \bar{K}^*(892)^0 \to K^0_S\pi^0$	$0.250\pm0.012\pm0.015^{+0.025}_{-0.024}$
$\bar{K}^*_0(1430)^0\pi^+, \bar{K}^*_0(1430)^0 \to K^0_S\pi^0$	$0.26\pm0.04\pm0.05\pm0.06$
$\bar{K}^*(1680)^0\pi^+, \bar{K}^*(1680)^0 \to K^0_S\pi^0$	$0.09\pm0.01\pm0.05^{+0.04}_{-0.08}$
$\bar{\kappa}^0\pi^+, \bar{\kappa}^0 \to K^0_S\pi^0$	$0.54\pm0.09\pm0.28^{+0.36}_{-0.19}$
$NR+\bar{\kappa}^0\pi^+$	$1.30\pm0.12\pm0.12^{+0.12}_{-0.30}$
$K^0_S\pi^0$ $S-$ware	$1.21\pm0.10\pm0.16^{+0.19}_{-0.27}$

At present, among the 3 angles of CKM triangle, α/ϕ_2, β/ϕ_1 and γ/ϕ_3, the γ/ϕ_3 is the least precisely measured mostly due to systematic uncertainty. The γ/ϕ_3 can be constrained by the phase differences c_i and s_i of D^0 and $\bar{D}^0$. Here, c_i and s_i denote the weighted average of $\cos\Delta\delta_D$ and $\sin\Delta\delta_D$, where $\Delta\delta_D$ is the phase difference of D^0 and $\bar{D}^0$. We perform binned Dalitz plot analysis of $D^0 \to K^0_{S/L}\pi^+\pi^-$ by using the flavored tags $K^-\pi^+$, $K^-\pi^+\pi^0$ and $K^-\pi^+\pi^+\pi^-$, the CP even tags K^+K^-, $\pi^+\pi^-$, $K^0_S\pi^0\pi^0$ and $K^0_L\pi^0$, as well as the CP odd tags $K^0_S\pi^0$, $K^0_S\eta(\gamma\gamma)$, $K^0_S\eta(\pi^+\pi^-\pi^0)$, $K^0_S\omega(\pi^+\pi^-\pi^0)$ and $K^0_S\eta'$ [20]. The extracted c_i and s_i with only statistical uncertainties are compared to the CLEO measurement [21] and the model prediction in Fig. 6. Our results represent a significant statistical improvement over previous measurements, which will allow for increased precision in the measurement of the unitarity triangle γ/ϕ_3 using the decay $B^\pm \to D(K^0_S\pi^+\pi^-)K^\pm$ through the GGSZ method [22].

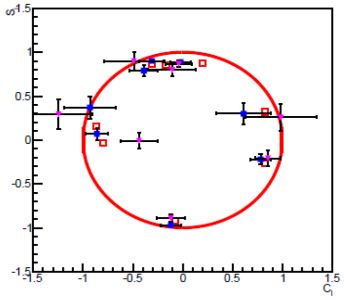

Fig. 6. The extracted s_i versus c_i from $D \to K^0_{S/L}\pi^+\pi^-$. The blue dot, pink triangle and red rectangle represent BESIII, CLEO and model prediction, respectively.

We determine the $D^0\bar{D}^0$ mixing parameter $y_{\rm CP} = (-2.1\pm1.3_{\rm stat.}\pm0.7_{\rm sys.})\%$, by analysis of $D^0 \to K^-\ell^+\nu_\ell$ ($\ell = e$ and μ) using the CP even tags K^+K^-, $\pi^+\pi^-$ and $K^0_S\pi^0\pi^0$, and the CP odd tags $K^0_S\pi^0$, $K^0_S\eta$ and $K^0_S\omega$ [23]. This result is compatible with the previous measurement with about two standard deviations. However, the precision is still statistically limited and less precise than the current world average.

Measurement of the strong phase difference between D^0 and $\bar{D}^0$ is important to relate to the $D^0\bar{D}^0$ mixing parameters x and y from x' and y'. We measure the $D \to K^-\pi^+$ strong phase difference based on analysis of $D^0 \to K^-\pi^+$ and $K^+\pi^-$ using the CP even tags K^+K^-, $\pi^+\pi^-$, $K^0_S\pi^0\pi^0$, $\pi^0\pi^0$ and $\rho^0\pi^0$, and the CP odd tags $K^0_S\pi^0$, $K^0_S\eta$ and $K^0_S\omega$ [24]. We determine the asymmetry of $\mathcal{A}^{\rm CP}_{K\pi}$ of the branching fraction of $D \to K^-\pi^+$ in CP-odd and CP-even eignensates to be $(12.7\pm1.3\pm0.7)\%$. With external inputs of $r^2 = (3.50\pm0.04)\times10^{-3}$, $y = (6.7\pm0.9)\times10^{-3}$ from HFAG [25] and $R_{WS} = (3.80\pm0.05)\times10^{-3}$ from PDG [19]. The $\cos\delta_{K\pi}$ is determined to be $1.02\pm0.11_{\rm stat.}\pm0.06_{\rm sys.}\pm0.01_{\rm input}$.

It is expected that $\mathcal{B}(D^{0(+)} \to \omega\pi^{0(+)})$ is at 10^{-4} level [26]. CLEO searched for and did not observe the $D^0 \to \omega\pi^0$ and $D^+ \to \omega\pi^+$ signals using single tag method [27]. They set the upper limits on these two decay branching fractions to be 2.6×10^{-4} and 3.4×10^{-4} at 90% confidence level, respectively. We search for $D^0 \to \omega\pi^0$ and $D^+ \to \omega\pi^+$ by using double tag method [28] with the fitted $\pi^+\pi^-\pi^0$ invariant mass spectra shown in Fig. 7. The significance of the $D^0 \to \omega\pi^0$ and $D^+ \to \omega\pi^+$ signals are 4.1σ and 5.4σ, respectively. These two branching fractions are determined to be $\mathcal{B}(D^0 \to \omega\pi^0) = (1.05\pm0.41_{\rm stat.}\pm0.09_{\rm sys.})\times10^{-4}$ and $\mathcal{B}(D^+ \to \omega\pi^+) = (2.74\pm0.58_{\rm stat.}\pm0.17_{\rm sys.})\times10^{-4}$. Also, we confirm that the ω helicity angle of the $D^{0(+)} \to \omega\pi^{0(+)}$ candidates follow the expected $H^2_\omega = \cos^2\theta_{\rm helicity}$ formalism.

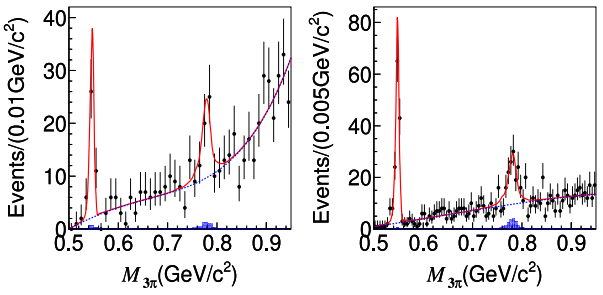

Fig. 7. Fits to the $\pi^+\pi^-\pi^0$ invariant mass spectra of the selected (Left) $D^0 \to \omega\pi^0$ and (Right) $D^+ \to \omega\pi^+$. The blue hatched hitograms are the sideband background events.

4 D rare decays

Search for the FCNC and LNV rare decays of charmed mesons can shed some lights on new physics beyond the SM. At BESIII, we have searched for the rare decays of $D^0 \to \gamma\gamma$ [29] and $D^+ \to K(\pi)^\pm e^\mp e^+$ [30] with double and single tag methods, respectively. No significant signals are observed, thus we set the upper limits of their branching fractions to be $\mathcal{B}(D^0 \to \gamma\gamma) < 3.8 \times 10^{-6}$, $\mathcal{B}(D^+ \to K^+e^+e^-) < 1.2 \times 10^{-6}$, $\mathcal{B}(D^+ \to K^-e^+e^+) < 0.6 \times 10^{-6}$, $\mathcal{B}(D^+ \to K^+e^+e^-) < 0.3 \times 10^{-6}$, $\mathcal{B}(D^+ \to K^-e^+e^+) < 1.2 \times 10^{-6}$ at 90% confidence level. Some of them are improved compared to previous measurements.

5 Λ_c^+ decays

The Λ_c^+ was observed in e^+e^- annihilation at Mark II in 1979 [31]. Thereafter, many works have been done to study the Λ_c^+ decay properties. However, the knowledge of Λ_c^+ physics are still very poor [5]. The sum of the branching fractions of the known Λ_c^+ decays is not more than 60% and their uncertainties are large. So, significantly improved measurements of these decay branching fractions are important to comprehensively understand the Λ_c^+ decay properties. By analysis of 567 pb^{-1} data taken at 4.559 GeV with the BESIII detector, we study 12 hadronic decays of Λ_c^+, which are $\Lambda_c^+ \to pK_S^0$, $pK^-\pi^+$, $pK_S^0\pi^0$, $pK_S^0\pi^+\pi^-$, $\Lambda\pi^+$, $\Lambda\pi^+\pi^0$, $\Lambda\pi^+\pi^+\pi^-$, $pK^-\pi^+\pi^0$, $\Sigma^0\pi^+$, $\Sigma^+\pi^0$, $\Sigma^+\pi^+\pi^-$ and $\Sigma^+\omega$ [32]. Fig. 8 shows the fits to the $M_{\rm BC}$ spectra of the accepted single tag candidates. From these, we obtain about 15 thousands of the singly tagged Λ_c^+ baryons.

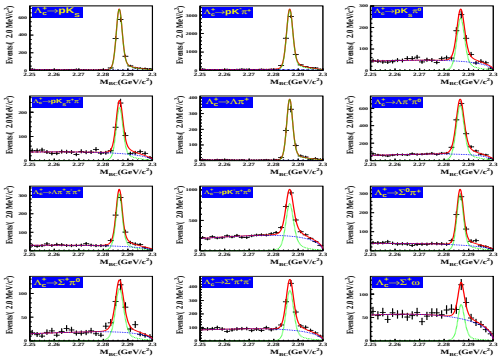

Fig. 8. Fits to the $M_{\rm BC}$ spectra of singly tagged $\Lambda_c^+ \to pK_S^0$, $pK^-\pi^+$, $pK_S^0\pi^0$, $pK_S^0\pi^+\pi^-$, $\Lambda\pi^+$, $\Lambda\pi^+\pi^0$, $\Lambda\pi^+\pi^+\pi^-$, $pK^-\pi^+\pi^0$, $\Sigma^0\pi^+$, $\Sigma^+\pi^0$, $\Sigma^+\pi^+\pi^-$ and $\Sigma^+\omega$.

At the recoil systems of the singly tagged Λ_c^+ baryons, we select the candidates for the doubly tagged $\Lambda_c^+\bar{\Lambda}_c^-$ baryon pairs. Fig. 9 shows the fits to the $M_{\rm BC}$ spectra of the accepted candidates. From these, we obtain about one thousand of the doubly tagged $\Lambda_c^+\bar{\Lambda}_c^-$ baryon pairs.

By combining the singly tagged Λ_c^+ baryons and the doubly tagged $\Lambda_c^+\bar{\Lambda}_c^-$ baryon pairs, we determine the absolute branching fractions of these twelve decays, which are $\mathcal{B}(\Lambda_c^+ \to pK_S^0) = (1.48 \pm 0.08)\%$, $\mathcal{B}(\Lambda_c^+ \to pK^-\pi^+) = (5.77 \pm 0.27)\%$, $\mathcal{B}(\Lambda_c^+ \to pK_S^0\pi^0) = (1.77 \pm 0.12)\%$, $\mathcal{B}(\Lambda_c^+ \to pK_S^0\pi^+\pi^-) = (1.43 \pm 0.10)\%$, $\mathcal{B}(\Lambda_c^+ \to pK^-\pi^+\pi^0) = (4.25 \pm 0.10)\%$, $\mathcal{B}(\Lambda_c^+ \to \Lambda\pi^+) = (1.20 \pm 0.67)\%$, $\mathcal{B}(\Lambda_c^+ \to \Lambda\pi^+\pi^0) = (6.70 \pm 0.35)\%$, $\mathcal{B}(\Lambda_c^+ \to \Lambda\pi^+\pi^+\pi^-) = (3.67 \pm 0.23)\%$, $\mathcal{B}(\Lambda_c^+ \to \Sigma^0\pi^+) = (1.28 \pm 0.68)\%$, $\mathcal{B}(\Lambda_c^+ \to \Sigma^+\pi^0) = (1.18 \pm 0.11)\%$, $\mathcal{B}(\Lambda_c^+ \to \Sigma^+\pi^+\pi^-) = (3.58 \pm 0.22)\%$ and $\mathcal{B}(\Lambda_c^+ \to \Sigma^+\omega) = (1.47 \pm 0.18)\%$, where the uncertainties are only statistical. These results are more precise than the PDG values [5]. The $\mathcal{B}(\Lambda_c^+ \to pK^-\pi^+)$ measured in this wok and the one measured at BELLE [33] will calibrate other decay rates of Λ_c^+ with much better precisions.

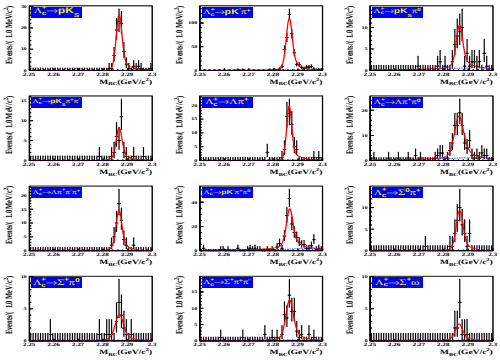

Fig. 9. Fits to the $M_{\rm BC}$ spectra of doubly tagged $\Lambda_c^+ \to pK_S^0$, $pK^-\pi^+$, $pK_S^0\pi^0$, $pK_S^0\pi^+\pi^-$, $\Lambda\pi^+$, $\Lambda\pi^+\pi^0$, $\Lambda\pi^+\pi^+\pi^-$, $pK^-\pi^+\pi^0$, $\Sigma^0\pi^+$, $\Sigma^+\pi^0$, $\Sigma^+\pi^+\pi^-$ and $\Sigma^+\omega$.

We also perform the first absolute measurement of the semileptonic decay of $\Lambda_c^+ \to \Lambda e^+\nu_e$ [34]. The $U_{\rm miss}$ distribution of the selected candidates is shown in Fig. 10. After subtracting background, we obtain 103.5±10.9 signal events of $\Lambda_c^+ \to \Lambda e^+\nu_e$. This leads to the absolute branching fraction to be $\mathcal{B}(\Lambda_c^+ \to \Lambda e^+\nu_e) = (3.63 \pm 0.38 \pm 0.20)\%$. This work improves the precision of the world average value [5] more than twofold. As the theoretical predictions on this rate vary in a large range of (1.4-9.2)%, this measurement provides a stringent test on these models.

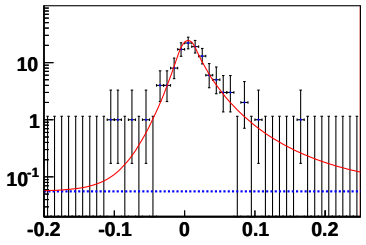

Fig. 10. $U_{\rm miss}$ distribution of the selected $\Lambda_c^+ \to \Lambda e^+\nu_e$ candidates.

6 Summary

In conclusion, by analyzing 2.93 and 0.567 fb^{-1} data taken at $\sqrt{s} = 3.773$ and 4.599 GeV with the BESIII detector, we report the precise measurements of the decay constant f_{D^+}, the form factors of D semileptonic decays, the Dalitz plot analysis of $D^+ \to K^0_S\pi^+\pi^0$, the strong phase differences in $D \to K^0_{S/L}\pi^+\pi^-$ and $K^-\pi^+$, the $D^0\bar{D}^0$ mixing parameter $y_{\rm CP}$, the searches for 2-body hadronic decays $D^{0(+)} \to \omega\pi^{0(+)}$, rare decays of $D^0 \to \gamma\gamma$ and $D^+ \to K(\pi)^\pm e^\mp e^+$ as well as the significant improved measurements of the absolute branching fractions for $\Lambda_c^+ \to \Lambda e^+\nu_e$ and 12 hadronic final states. These are important to test the LQCD calculations on f_{D^+} and the form factors of D semileptonic decays, to test the CKM matrix unitarity, to search for new physics beyond the SM, and to comprehensively understand the Λ_c^+ decay property. In 2016, BESIII will collect 3 fb^{-1} data at 4.18 GeV. More interesting physics based on charmed mesons and charmed baryons are hopefully achieved at BESIII in the near future.

References

1 M. Ablikim, *et al.* (BESIII Collaboration), Nucl. Phys. Meth. A 614, 345 (2010).
2 M. Ablikim, *et al.* (BESIII Collaboration), Chin. Phys. C 37, 123001 (2013).
3 M. Ablikim, *et al.* (BESIII Collaboration), Chin. Phys. C 39, 093001 (2015).
4 M. Ablikim, *et al.* (BESIII Collaboration), Phys. Rev. D 89, 051104(R) (2014).
5 K. A. Olive, *et al.* (Particle Data Group), Chin. Phys. C 38, 090001 (2014).
6 B. I. Eisenstein, *et al.* (CLEO Collaboration), Phys. Rev. D 78, 052003 (2008).
7 E. Follana, *et al.* (HPQCD and UKQCD Collaborations), Phys. Rev. Lett. 100, 062002 (2008).
8 M. Ablikim, *et al.* (BESIII Collaboration), Phy. Rev. D 92 (2015) 072012.
9 D. Becirevic and A. B. Kaidalov, Phys. Lett. B 478, 417 (2000).
10 T. Becher, R. J. Hill, Phys. Lett. B 633, 61 (2006).
11 H. Na, *et al.* (HPQCD Collaboration), Phys. Rev. D 82, 114506 (2010).
12 H. Na, *et al.* (HPQCD Collaboration), Phys. Rev. D 84, 114505 (2010).
13 M. Ablikim, *et al.* (BESIII Collaboration), arXiv:1510.00308[hep-ex], submitted to Phys. Rev. D.
14 Fenfen An (For BESIII Collaboration), arXiv:1509.03932, Hailong Ma (For BESIII Collaboration), arXiv:1509.04424, proceedings of the talks presented at Charm2015.
15 J. G. Korner and G. A. Schuler, Z. Phys. C 46, 93 (1990); F. J. Gilman and R. L. Singleton, Jr., Phys. Rev. D 41, 142 (1990).
16 J. M. Link, *et al.* (FOCUS Collaboration), Phys. Lett. B 54 544, 89 (2002).
17 M. Ablikim, *et al.* (BESIII Collaboration), Phy. Rev. D 92 (2015) 071101.
18 M. Ablikim, *et al.* (BESIII Collaboration), Phys. Rev. D 89, 052001 (2014).
19 J. Beringer, *et al.* (Particle Data Group), Phys. Rev. D 86, 010001 (2012).
20 Dan Ambrose (For BESIII Collaboration), talk presented at APS2014.
21 R. A. Briere, *et al.* (CLEO Collaboration), Phys. Rev. D 80, 032002 (2009); J. Libby, *et al.* (CLEO Collaboration), Phys. Rev. D 82, 112006 (2010).
22 A. Giri, *et al.*, Phys. Rev. D 68, 054018 (2003).
23 M. Ablikim, *et al.* (BESIII Collaboration), Phys. Lett. B 744, 339 (2015).
24 M. Ablikim, *et al.* (BESIII Collaboration), Phys. Lett. B 734, 227 (2014).
25 Heavy Flavor Averaging Group, http://www.slac.stanford.edu/xorg/hfag/charm/.
26 Hai-Yang Cheng and Cheng-Wei Chiang, Phys. Rev. D 81, 074021 (2010).
27 P. Rubin, *et al.* (CLEO Collaboration), Phys. Rev. Lett. 96, 081802 (2006).
28 Hajime Muramatsu (For BESIII Collaboration), arXiv:1510.00308[hep-ex], proceeding of the talk presented at Charm2015.
29 M. Ablikim, *et al.* (BESIII Collaboration), Phy. Rev. D 91 (2015) 112015.
30 Minggang Zhao (For BESIII Collaboration), talk presented at Charm2015.
31 G. S. Abrams, *et al.* [Mark II Collaboration], Phys. Rev. Lett. 44, 10 (1980).
32 Xiaorui Lv (For BESIII Collaboration), talk presented at Charm2015.
33 A. Zupanc, *et al.* (Belle Collaboration), Phys. Rev. Lett. 58 113, 042002 (2014).
34 M. Ablikim, *et al.* (BESIII Collaboration), Phy. Rev. Lett. 115 (2015) 221805.